Effect of long duration UV irradiation on diamondlike carbon surfaces in the presence of a hydrocarbon gaseous atmosphere

A. Riedo,[a] P. Wahlström, J. A. Scheer, P. Wurz, and M. Tulej
Physics Institute, University of Bern, Sidlerstrasse 5, CH-3012 Bern, Switzerland

(Received 28 June 2010; accepted 23 October 2010; published online 13 December 2010)

Measurements of the effect of long duration UV irradiation (up to 2905 min) of flight quality diamondlike carbon charge state conversion surfaces for application in space research in the presence of a hydrocarbon atmosphere were done. An isopropanol atmosphere was used for simulating the hydrocarbon gaseous environment for an instrument on a satellite in space. Charge state conversion surfaces are used in neutral particle sensing instruments where neutral atoms have to be ionized prior to the analysis. A narrow-band (126 ± 5 nm) discharge lamp and a broad-band deuterium lamp (112–370 nm) were used as sources of UV radiation. The UV irradiation of a surface results in the desorption of some volatiles present on the surface and the decomposition of others. Desorption of volatiles, mostly water, is observed for both UV sources. The decomposition of the hydrocarbons and the subsequent build-up of a hydrocarbonaceous layer is only observed for the broad-band UV lamp, which is more representative for the space environment. Unfortunately, the hydrocarbonaceous layer cannot be removed thermally, i.e., it is permanent, and causes a degradation of the performance of the charge state conversion surfaces. With the present measurements we can quantify the UV influence at which the degradation of the conversion surfaces becomes noticeable. © *2010 American Institute of Physics*. [doi:10.1063/1.3517832]

I. INTRODUCTION

The interaction of atomic and molecular particles with insulating surfaces has been researched extensively in recent years.[1–10] Reports of relatively high fractions of negative ions resulting from scattering of positive atomic and molecular ions off insulating surfaces suggested possibilities for several new applications. Among these applications, we use this process in instruments on spacecraft for efficient detection of 10 eV–2 keV neutral atoms originating in interplanetary or interstellar space.[11–13] This detection technique has already been successfully employed in several satellite missions, such as in the IMAGE and the more recent IBEX satellite mission.[9,10,14–16]

Due to internal out gassing from the actual instrument and also from spacecraft components during the mission,[17] a hydrocarbon gaseous environment for the instrument and therefore for the surfaces is expected as has been observed on previous missions.[17] From previous laboratory measurements and observations it is known that UV irradiation will cause dissociation of organic molecules.[18–20] The remaining fragments of the molecules on the surface then build up as stable layers on such surfaces (carbonation), which cannot be removed anymore by simply heating the surfaces. Similar findings are reported in Refs. 21 and 22 where UV polymerization of hydrocarbon contaminants onto optical surfaces was measured, resulting in a degradation of the filter transmission. From this point of view, and especially for the future mission BepiColombo where at Mercury's distance the UV irradiation is up to ten times higher than at 1 AU,[23,24] a long duration measurement became necessary to understand the effect of UV irradiation on conversion surfaces (CS). Therefore, further investigations into conversion surface properties, such as the ability to convert neutral atoms to negatively charged ions (conversion efficiency) and the angular scattering, were done. The latter is important because a low spread of scattering angles minimizes scattered particle loss in downstream ion-optical analyzer systems. A low spread of angular scattering and a high ionization yield are the two key requirements for successful conversion surface performance in a space instrument.

Interstellar gas consists mainly of H and He with minor fractions of O, N, C, and Ne.[25] To optimize the sensitivity of these measurements we focused on O and Ne. In the case of oxygen, atomic and molecular ions were used. The impact of using positively charged atomic and molecular ions on the results is discussed in detail later.

The scattering measurements were done at moderate vacuum conditions, i.e., in the low 10^{-7} mbar range, which mirror the conditions within a typical particle sensing instrument on a satellite shortly after launch. From the European Space Agency's ROSETTA mission it is known that several weeks after launch, the pressure in the vicinity of the spacecraft drops to the low 10^{-9} mbar range, and into the 10^{-10} mbar range after few months.[17,26] The pressure inside space instruments with small openings to vent to the outside, such as most particle instruments, is expected to be at least an order of magnitude higher than the pressure outside the spacecraft. Because of internal outgassing, pressures in the 10^{-8} mbar range are expected to persist in space particle instruments more or less indefinitely.

[a]Electronic mail: riedo@space.unibe.ch.

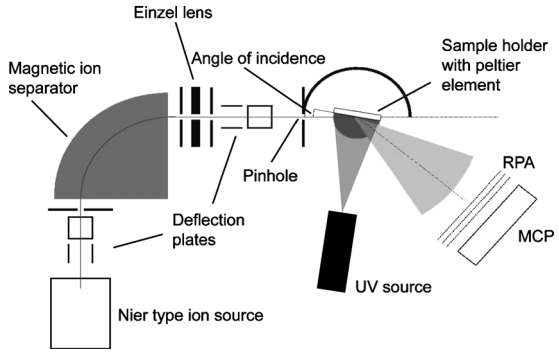

FIG. 1. Schematic overview of the ILENA apparatus at the University of Bern. Positive ions are extracted from a Nier type ion source and after being mass analyzed they are scattered from the DLC sample. The distribution of scattered particles is finally recorded with a 2D imaging MCP detector.

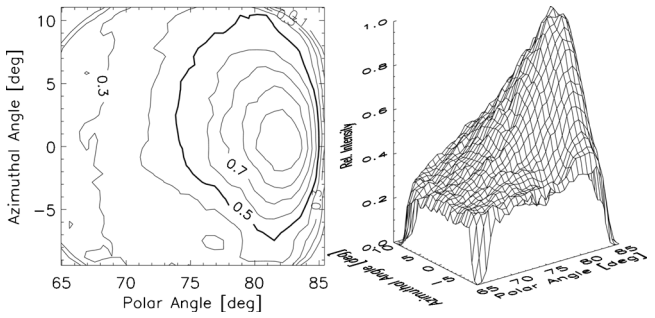

FIG. 2. Left: contour plot of the angular scattering distribution of 1000 eV Ne^+ recorded by the imaging MCP detector after an UV irradiation time of 2 min by using the broad-band deuterium lamp. The bold line indicates the 50% level. Right: same data displayed in three-dimensions.

II. EXPERIMENT

The surfaces tested are diamondlike carbon (DLC) charge state conversion surfaces, which are tetrahedral amorphous-carbon (ta-C) films on silicon single crystal substrates. The ta-C films have a high fourfold (i.e., sp^3) content measured at >80% of the amorphous films.[10] The surface roughness is less then 3 Å rms, measured with an AFM. More information can be found in Ref. 10.

Particle scattering measurements were made with the imager for low energetic neutral atoms (ILENA) apparatus at the University of Bern, Switzerland. Figure 1 displays an overview of the ILENA experimental setup. The energy range of incident particles chosen for these measurements was 390–1000 eV. For all measurements the angle of incidence was 6° with respect to the surface normal. The scattering angle was identified by rotating the detector to maximize the scattered peak. The experimental setup will be described briefly below, more details on the experimental setup can be found in Refs. 11 and 27.

The ILENA apparatus consists of an ion source, a magnetic ion separator providing a mass resolution of $m/\Delta m \approx 45$, an ion beam guiding system, a sample stage with housing and a detection unit. The sample is mounted on a Peltier cooling element to keep the sample at a low temperature of about 0 °C. The low temperature helps to accumulate the isopropanol test gas on the surface more efficiently when the UV source is irradiating the sample. All these units are contained in a single vacuum chamber pumped by an ion getter pump. The reflected beam is recorded using a two-dimensional (2D) position-sensitive multichannel plate (MCP) detector with a viewing angle of ±12.5° in both, azimuthal and polar direction.

A typical measurement of the angular scatter distribution is shown in Fig. 2. A retarding potential analyzer (RPA) consisting of three grids is mounted in front of the MCP detector. The detector unit, including the RPA, is shielded electrostatically and can be rotated independently from the converter surface around the same axis. The outer grids of the RPA are grounded to shield the inner grid, which can be biased to suppress ions. An additional grid in front of the MCP detector at negative potential with respect to the MCP detector serves to reject secondary electrons originating from the preceding grids and the converter surface. The MCP detector may be floated at a high negative voltage to vary the transmission threshold for negative particles. After baking out the vacuum chamber at 80 °C for several hours, a residual gas pressure in the mid 10^{-8} mbar range is achieved. During operation the pressure may rise into the low 10^{-7} mbar range as a result of test gas leaking into the ion source chamber.

The fraction of negative ions is determined by taking measurements with and without an applied floating voltage on the MCP detector. In the first case, only neutral particles are recorded, in the latter case neutral particles and negative ions are recorded simultaneously. The difference gives the fraction of negative ions. Each data-point results from a series of successive measurements, which allows the registration of ion beam drifts and possible surface charging during each measurement series. With the MCP detector, it is not possible to distinguish between scattered and negatively ionized primary oxygen particles and sputtered negative ions from the conversion surface. Therefore, neon without the ability to form negative ions and with a comparable mass to oxygen was taken as a proxy to assess the background of sputtered negative ions for the evaluation of the negative ionization yield of atomic and molecular oxygen. The sputtered fractions were finally subtracted from the negative ionization yields of oxygen. Oxygen was chosen because it allows for a sensitive measurement of deteriorating effects on the conversion surface. The detection efficiency of the MCP is taken from Refs. 28 and 29, where an identical detector was used.

Two different UV light sources for the measurements were used to irradiate the conversion surface for different total irradiation times with the conversion surface being in the isopropanol environment. For the first measurement campaign, a dielectric barrier discharge excimer lamp filled with Ar gas, having a central wavelength of 126 ± 5 nm (manufacturer USHIO Lighting Edge Technologies, Japan) is used. The source intensity amounts to 31.4×10^{-3} W/cm^2 (1.96×10^{16} ph/cm^2 s), measured at the conversion surface location in the ILENA facility with a National Institute of Standards and Technology (NIST)-calibrated photodiode (Diode: SXUV100; International Radiation Detectors, Inc., California). Measurements were done up to a total irradiation time of 2905 min. Because no changes in surface properties were

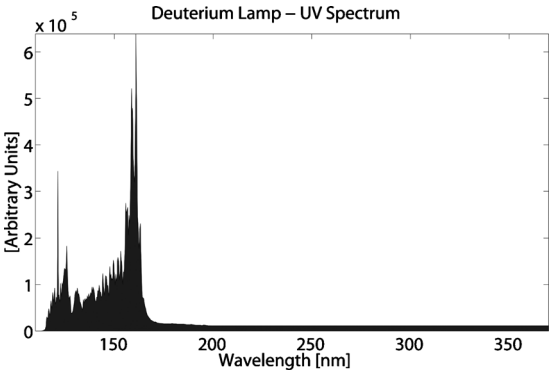

FIG. 3. UV spectrum of the broad-band deuterium lamp in the range of 112–370 nm.

found, a second measurement campaign was performed by using a deuterium lamp (manufacturer Cathodeon Ltd. Cambridge, Type F05, England) with a broader UV spectrum in the range of 112–370 nm (Fig. 3). The used UV source has an intensity of 4.4×10^{-4} W/cm^2 (3.65×10^{14} ph/cm^2 s), measured at the conversion surface location in the ILENA facility with a NIST-calibrated photodiode. Measurements were done up to a total irradiation time of 1440 min.

After each UV irradiation cycle, the UV source was switched off and the evaporation of isopropanol was stopped. In the following, surface scattering measurements of oxygen as well as of neon ion beams were performed. After the measurements, the ion source was switched off and the next cycle of UV irradiation in the presence of isopropanol was commenced.

Laser-desorption mass spectra with the laser time-of-flight mass spectrometer (LMS) apparatus at the University of Bern, Switzerland, of clean and irradiated samples were done.[20] Laser fluences near the desorption threshold[30] for molecular ion desorption were chosen to investigate the chemical composition of the surface contamination. This allowed for the further investigation of the composition of the accumulated hydrocarbonaceous crust accumulated on the CS during the UV campaign using the deuterium lamp as UV source. Mass spectra of the contaminated and of a new and uncontaminated CS were done under almost identical experimental conditions.

The LMS apparatus consist of a Q-Switched Nd:yttrium aluminum garnet (YAG) laser and a reflectron time of flight (RTOF) mass spectrometer. The Nd:YAG laser is operated at 20 Hz with a wavelength of 266 nm, with laser intensities selected for molecular desorption.[30] The RTOF is contained in a single vacuum chamber pumped by an ion getter pump. All measurements were done in the mid 10^{-8} mbar range. More details on the experimental setup can be found in Ref. 20.

III. RESULTS

Although we eventually want to detect neutral atoms in space, we used for the first measurement campaign positive molecular ions and for the second measurement campaign atomic ions. Positive ions were used instead of neutrals because they can be produced far more efficiently, and with much better energy, intensity and angle control in our system than can neutrals. But the charge and, for the first measurement campaign, the use of molecules, must be justified.

From previous experiments with several other insulating surfaces [polycrystalline diamond,[11] single-crystal diamond,[31,32] and MgO (Ref. 12)] it has been established that incident hydrogen and oxygen ions are effectively neutralized upon scattering. These previous measurements were done with both incident positive ions and with incident neutral particles and they revealed the same negative ion fractions in both cases. As a result, we can assume complete memory loss of the incident charge state after scattering.

The use of molecules instead of atoms is justified as follows. A molecule has many more electronic states than an atom, so we cannot expect the charge exchange process while scattering to be identical. But according to Refs. 10 and 11, more than 80% of molecules with energy in the 300–1000 eV range, when scattered off a polycrystalline diamond surface, dissociate shortly before reaching the surface, on the incoming leg of the trajectory. That means that the final charge state fraction is determined mainly by charge exchange processes between the surface and dissociated atoms. Therefore, we conclude that the use of molecules causes a negligible change to the charge state fractions measured in this study. After all, here we are only interested in a change in the performance of the conversion surface upon UV irradiation in a hydrocarbon environment.

Significant changes in surface properties were only found by using the deuterium lamp. To compare the Deuterium lamp with the solar UV radiation in the pertaining UV range of 112–370 nm, we measured the total UV source intensity of 4.4×10^{-4} W/cm^2 (3.65×10^{14} ph/cm^2 s). The Sun contributes in this UV range approximately 5.5% of the solar constant (S_{tot}=1367 W/m^2),[33,34] which is 7.5×10^{-3} W/cm^2. Therefore, the conversion factor between the UV source and the Sun at 1 AU amounts to 1/17. The UV intensity of the Sun scales quadratically with the location of Mercury. At the perihelion (S_{tot}=14470 W/m^2) the UV intensity is more than ten times higher than at 1 AU,[23,24] which decreases the conversion factor between the UV source and at Mercury's location to 1/170. The narrow-band discharge lamp, having a central wavelength of 126 ± 5 nm, has a measured total UV intensity of 31.4×10^{-3} W/cm^2 (1.96×10^{16} ph/cm^2 s). The photon flux of the Sun in this UV range at 1 AU, regarding the Lyman-α radiation of the hydrogen emission at 121.6 nm, amounts to about 5×10^{11} ph/cm^2 s (8.2×10^{-7} W/cm^2).[35] Therefore, the conversion factor between the narrow-band UV source and the Sun at 1 AU amounts to about 3.8×10^4, at Mercury's location to 3.8×10^3, respectively.

A. Angular scattering

The direction of angular deviation from specular scattering that resides in a plane containing the incoming trajectory and normal to the surface is defined as polar scattering. The direction of specular scattering normal to the polar angle plane is defined as azimuthal scattering, with zero indicating a true specular reflection (Fig. 2).

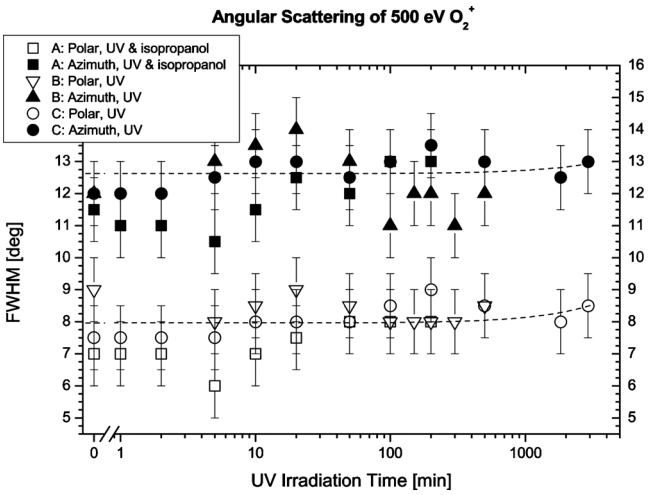

FIG. 4. Angular scattering (FWHM) as function UV irradiation time vs for of 500 eV O_2^+ using the narrow-band discharge lamp. Measurement uncertainties of ±1° for angular scattering. No significant changes in the angular scattering due to UV irradiation are visible. Furthermore, no significant differences between measurement campaign A and B, C are observed. Solid and dashed lines give linear regressions to the data of campaign C.

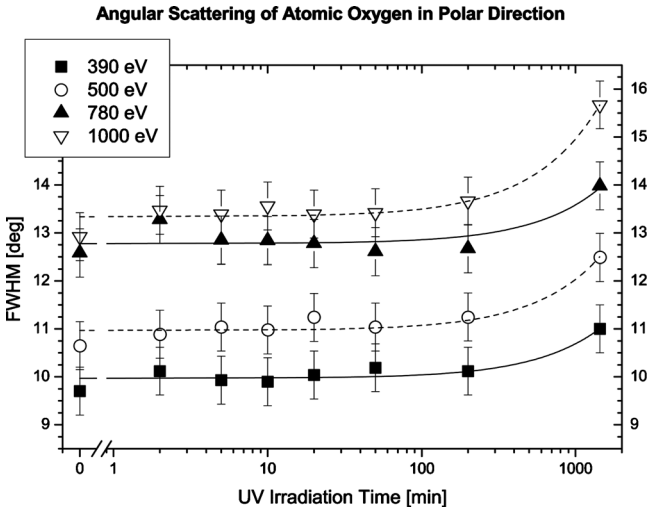

FIG. 5. Angular scattering (FWHM) in polar direction of atomic oxygen using the broad-band deuterium lamp. Measurement uncertainties of ±1° for angular scattering. Significant changes after UV exposure of 1440 min are visible. The solid and dashed lines represent linear regressions.

Figure 4 shows the angular scattering distributions of three measurement campaigns versus UV irradiation time by using excimer lamp. In the first campaign (A), surface A within an isopropanol atmosphere was used. In the second campaign (B), surface B was used, which is not immersed in an isopropanol atmosphere. In the third campaign (C), the measurements using surface B are repeated. But before these measurements were done, the vacuum chamber was vented to air to assure that campaign C has the same initial conditions as campaign B, except for the UV irradiation. The surfaces A and B are both DLC surfaces with similar surface properties, such as the capability to convert neutrals into negative ions or angular scattering properties. In campaign A, no significant changes in full width at half maximum (FWHM) in polar and azimuthal direction after UV irradiation are seen, within the measurement uncertainties of ±1°. Furthermore, no significant differences between the campaigns A, B, and C were recorded.

The situation is quite different when using the deuterium lamp as UV source in the presence of an isopropanol atmosphere. Figures 5 and 6 show the angular scatter (FWHM) versus UV irradiation time for oxygen and neon, respectively, for several energies. Up to an UV irradiation time of 200 min the measurements of FWHM of angular scattering in polar direction of atomic oxygen and neon show a slight increase in the FWHM with increasing UV irradiation time. However, the statistical analysis of these measurements shows that these measurements agree with the non-irradiated surface within the measurement uncertainties of ±0.5°. Significant changes in angular scattering are recorded only after UV irradiation time of 1440 min. The same trend is also observed in the neon measurements. At higher ion energies changes in FWHM of atomic oxygen are larger than those of neon.

B. Ionization yield

Figure 7 shows the negative ionization yield of 500 eV O_2^+, using the excimer lamp versus UV irradiation time for the three measurement campaigns A, B, and C. An increase in the negative ionization yields in all three measurement campaigns is seen with increasing UV irradiation time of up to 200 min, independent of the presence of isopropanol, within the error bars of ±1%. After 200 min the increase in negative ionization yield levels off at approximately 14%.

The negative ion fractions of atomic oxygen (Fig. 8), by using the deuterium lamp as UV source in the presence of an isopropanol atmosphere, are very similar to the measurements of molecular oxygen (Fig. 7), within the error bars of ±1%, where a significant increase in the negative ionization yield is observed upon prolonged UV irradiation. After each UV irradiation cycle the negative ionization yields increased. Due to the UV irradiation the negative ionization yield had increased from about 10% to 17% for lower ion energies and from 12% to 18% for higher ion energies, respectively (Fig. 8). In contrast to the ion fractions of atomic oxygen (Fig. 8),

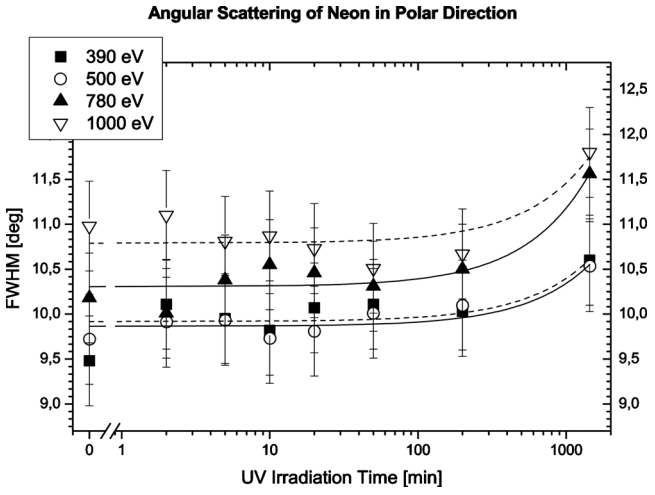

FIG. 6. FWHM of angular scattering in polar direction of neon using the broad-band deuterium lamp. Measurement uncertainties of ±0.5° for angular scattering. Significant changes occurred after UV irradiation time of 1440 min. The solid and dashed lines represent linear regressions.

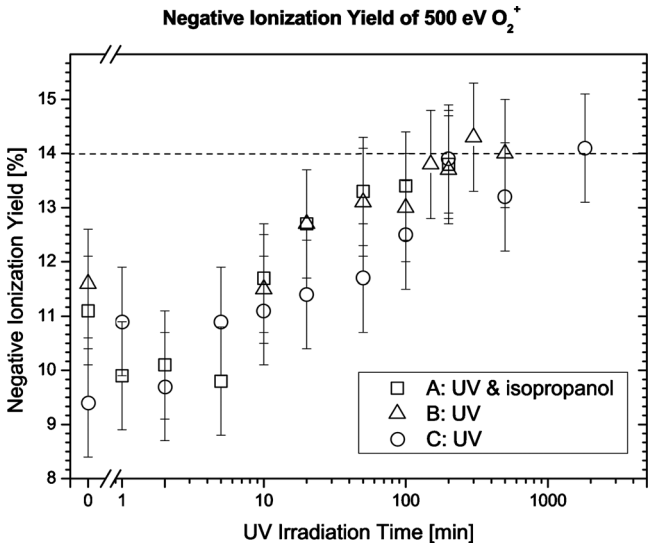

FIG. 7. Negative ionization yields of 500 eV O_2^+ of the three measurement campaigns A, B, and C by using the narrow-band discharge lamp. Measurement uncertainties of ±1% for negative ionization yield. The negative ionization yields begin to stagnate at about 14% (see dashed line). Sputtering background is subtracted.

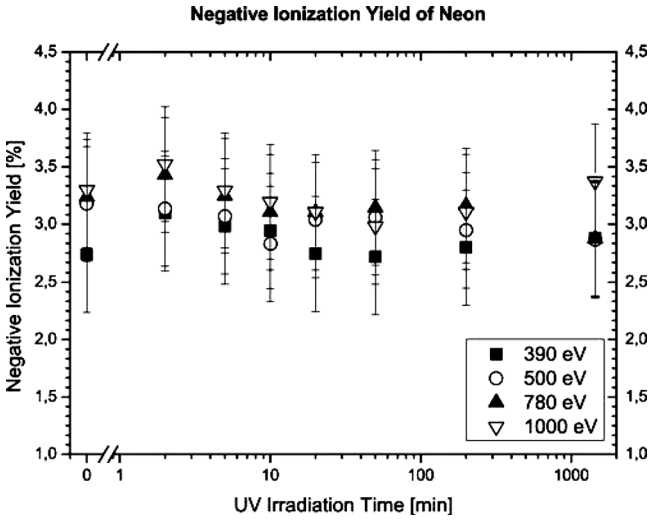

FIG. 9. Negative ionization yields of neon by using the broad-band deuterium lamp. Measurement uncertainties of ±0.5% for negative ionization yield. In contrast to the measurements of negative ionization yields of atomic oxygen using the broad-band deuterium lamp (Fig. 8), no increase in the yields after each UV irradiation cycle is measured.

no increase in the negative ionization yield for neon is seen with increasing UV irradiation, with measurement uncertainties of ±0.5% (Fig. 9).

C. Chemical composition of the accumulated hydrocarbonaceous crust

Because it is of great interest to know the composition of the accumulated layers during the UV campaign using the deuterium lamp as UV source, laser-desorption mass spectra of the contaminated and a new and uncontaminated CS were recorded under very similar experimental conditions. Spectra at different laser intensities starting from the threshold intensity for molecular ion desorption and upwards were used for the chemical identification of hydrocarbon compounds formed under UV irradiation.

Figure 10 shows the mass spectrum of the hydrocarbonaceous crust accumulated on the diamondlike CS during the UV irradiation using the deuterium lamp as UV source, recorded with a laser intensity near the threshold. Figure 11 shows the mass spectra of a new and uncontaminated CS under identical experimental conditions for laser desorption. In Fig. 10, a complex mass spectrum with masses up to 200 amu was recorded, which is in contrast to Fig. 11, where only the electronic background is visible. No sign of hydrocarbon molecules, or any other molecule, was found for the uncontaminated CS. This is expected, since the diamondlike

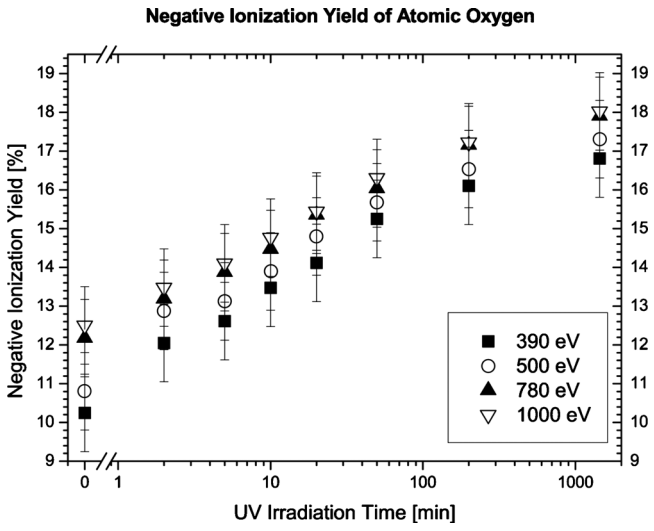

FIG. 8. Negative ionization yield of atomic oxygen by using the broad-band deuterium lamp. Measurement uncertainties of ±1% for negative ionization yield. Sputtering background is subtracted. After each UV irradiation cycle the negative ionization yields increased.

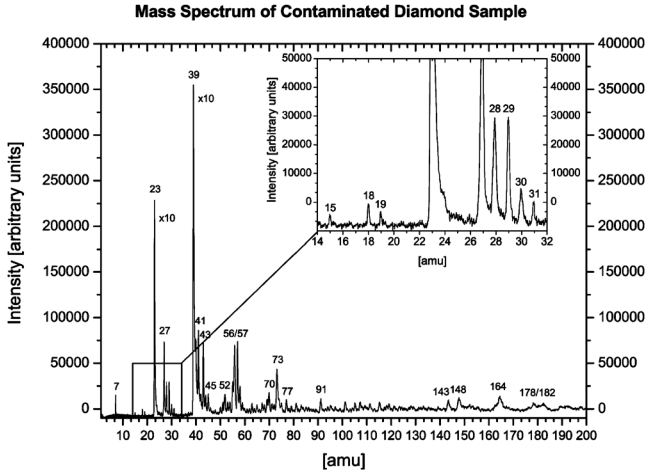

FIG. 10. Mass spectrum of the hydrocarbonaceous crust accumulated on the diamondlike CS during the UV campaign by using the deuterium lamp as UV source is shown, using laser intensities near threshold for ion desorption. On the top right of the figure, a blow-up of the mass range of 14 to 32 is displayed. Due to saturation of the intensity of the masses 23 and 39 both have to be thought ten times higher in intensity compared to the other masses as displayed in the figure.

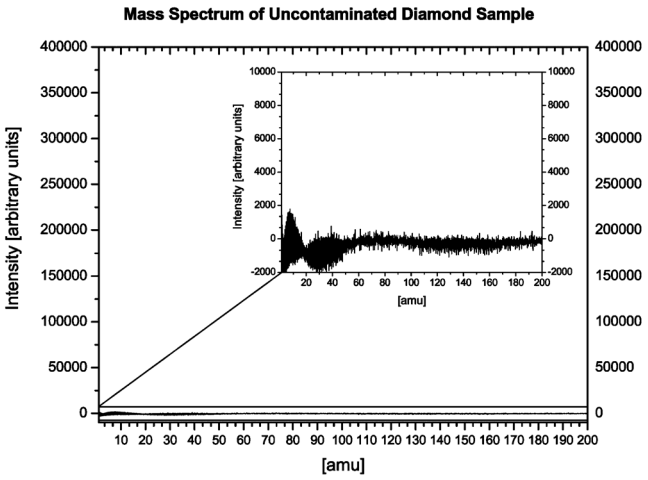

FIG. 11. Mass spectrum of a new and uncontaminated CS is shown for the same experimental conditions as used in Fig. 10. On the top right, a blow-up of the mass range of 1 to 200 amu is displayed. Only electronic background as measured, in stark contrast the measurements shown in to Fig. 10.

surface should be strong enough to withstand the low laser powers used in desorption mode without atoms or molecules being released from its surface. Moreover, since diamond is chemically inert, contamination by adsorbates should be minimal, if occurring at all. The contaminated and the uncontaminated samples were in air for a few weeks, before they were introduced into the LMS facility for the mass spectrometric measurements of the surface contamination. These measurements demonstrate that there is a permanent layer on the contaminated sample, which consists mostly of hydrocarbon molecules, which are likely produced by UV-induced polymerization of the isopropanol (C_3H_8O). Indications for this interpretation at lower masses are: mass 15 (CH_3^+), mass 27 ($C_2H_3^+$), mass 28 ($C_2H_4^+$), or mass 41 ($C_3H_5^+$). At higher masses: mass 56 ($C_4H_8^+$), mass 57 ($C_4H_9^+$), mass 70 ($C_5H_{10}^+$,$C_4H_6O^+$), mass 73 ($C_4H_9O^+$), or mass 91 ($C_7H_7^+$). The measured peak at the mass 19 is most probably protonated water (H_3O^+) and is likely a result from absorbed humidity of the laboratory air in the carbonaceous layer during the time when the CS was left outside the vacuum chamber. The masses 7 (Li+), 23, and 39, most probably Na^+ and K^+, are likely contaminants of isopropanol because isopropanol, often used as cleaning solvent, cannot be produced with such high purity. Furthermore, the measured high intensities of Li+ and the saturated peaks of Na^+ and K^+ are explainable through their low ionization potential and high ionization efficiencies. However, most of the measured masses are identified to be likely products of polymerization and fragmentations of isopropanol (C_3H_8O), namely hydrocarbon molecules, during the UV irradiation campaign using the deuterium lamp as UV source.

When interpreting the measured sequence of molecules observed in the mass spectrum of the contaminated sample (Fig. 10) fragmentation of the larger molecules accumulated on the surface during the laser desorption process has to be considered. When increasing the intensity of the desorption laser, we found that the signal increases sharply, but also the fragmentation increases, resulting in an increasing abundance of the smaller fragments. Thus, we can assume that the hydrocarbon layer on the surface consists of much larger, polymerized, hydrocarbon compounds. Similar findings are reported in Ref. 19 where the fragmentation of the C_{60} was investigated and observed by using laser beams and light in comparable UV ranges.

If the laser intensities are too high, a plasma is formed in front of the sample, where chemical processes occur in the plasma plume. Not only fragmentation occurs but also new chemical compounds may be formed in the plasma plume, masking the original chemical composition of the accumulated crust. These conditions are easily recognized and avoided for this analysis. Similar results are reported in Ref. 30 where the threshold energy for desorption of the C_{60} molecule was further investigated.

IV. DISCUSSION

Using the narrow-band discharge lamp we did not find any changes in the angular scattering of molecular oxygen with prolonged irradiation (Fig. 4), which we interpret that there was no build-up of a hydrocarbonaceous layer. However, we always observe an increase in the negative ionization yields (Fig. 7, campaigns A, B, and C). Thus, we can conclude that the narrow-band discharge lamp has only cleaned the surfaces. Most likely from water, which is the major part of the residual gas in the vacuum chamber. These observations are in good agreement with the specification of the narrow-band discharge lamp, which is actually intended as cleaning system for surfaces in the UHV environment.

The situation is different when using the broad-band deuterium lamp (112–370 nm). The negative ionization yields of atomic oxygen (Fig. 8) have increased after each UV irradiation cycle and also an increase in angular scattering of atomic oxygen and neon after the UV irradiation time of 1440 min was observed (Figs. 5 and 6). This observation can be explained as follows. On the one hand and like the narrow-band discharge lamp, the broad-band lamp has cleaned the surface, which is seen by the increase in the negative ionization yields of atomic oxygen and neon (Figs. 5 and 6). Again, most likely the surface is cleaned from water. On the other hand, and in contrast to the narrow-band discharge lamp, the photons of the lamp have enough energy to form superexcited molecules (vibrationally excited, doubly excited, or inner-core excited molecular high Rydberg states converging to each ion state).[36,37] Such molecules can decay into ions, by emitting an electron, or into radicals by dissociation.[36] The latter is for our consideration the most important channel for the build-up of carbonation layers and is supported by the laser-desorption mass spectra of the contaminated CS (Figs. 10 and 11). However, such hydrocarbonaceous layers will increase the surface roughness and therefore affect adversely properties of the conversion surface, such as the angular scattering and the ionization yield, which we observed in our measurements. This circumstance is again in good agreement with previous findings,[9,10,38] that higher surface roughness increases the probability for violent collisions and thus the probability for charge exchange processes.

In addition, we can generalize the problem of the

build-up of carbonation layers to other hydrocarbon molecules. The ionization efficiencies and therefore the probability of dissociation into radicals of other hydrocarbons increase all nearly in the same UV wavelength range of about 120–140 nm and increase by decreasing wavelength; the threshold of the ionization of isopropanol is at 120 nm.[36]

It is not explained yet, why no increase in negative ionization yield of neon (Fig. 9) after each UV irradiation cycle by using the broad-and deuterium lamp was measured. Neon as a noble gas cannot form negative ions and therefore we consider it as an upper limit of sputtering background of negative ions in the measurement of the negative ionization yields of molecular and atomic oxygen. The sputter yield of negative ions does not depend on UV irradiation.

We found increasing negative ionization yields of atomic oxygen with increasing energy of the incident ions (Fig. 8). Similar findings have been reported for other insulating surfaces such as LiF, MgO and $BaZrO_3$,[8,12,39] and we follow the same argumentation, that higher energies cause smaller distances of closest approach between impacting ions and surface atoms, which results in higher probabilities for charge exchange processes and thus yields higher fractions of negative ions.

Finally, it has to be explained how charge exchange happens when particles scatter off an insulating surface. According to Refs. 40 and 41, the width of the band gap of Al_2O_3 is about 9 eV. The negative electron affinity levels of H and O are 0.75 and 1.46 eV below the vacuum level, respectively. The valence band is filled and there is no electron mobility in an insulator. So one should not expect that charge exchange would be possible. But it has been found that for ionic crystals such as, for instance, LiF, charge exchange proceeds via capture of electrons from the anionic sites of the surface in a binary ion–atom interaction.[42–44] And once the negative ion is formed it cannot be destroyed by resonant electron loss (as in the case of metals) because of the band gap of the ionic crystal. It is safe to expect a similar behavior here. In addition, the probability for a particle to be negatively charged increases with increasing effective number of collisions, and thus at grazing incidence angles.

V. CONCLUSION

The motivation for this study was the question how solar UV irradiation changes the conversion surface properties in the presence of a hydrocarbon gaseous environment in an instrument on a satellite in space. The largest UV source is the Sun, but UV from planetary coronas can also give high UV fluxes into an instrument. Hydrocarbons are present in the spacecraft environment even after long durations in space.

Hydrocarbon compounds condensed on a surface will decompose to a hydrocarbonaceous layer upon intense UV irradiation. This hydrocarbonaceous layer cannot be removed thermally (i.e., heating the affected surface) and has to be considered permanent. The formation of permanent hydrocarbonaceous layers on walls of vacuum chambers upon intense UV irradiation is observed often, but so far its formation has not been quantified. After an irradiation time of 1 h at 1 AU, where the broad-band UV source has only 1/17 of the solar UV intensity in the pertaining UV range, the build-up of a permanent surface layer shows up in the data of angular scatter. The hydrocarbonaceous layer negatively affects the performance of the conversion surface. Furthermore, the irradiation time is cumulative; there is no recovery of the irradiated surface for shorter exposure times. At Mercury orbit, where the solar UV intensity is up to ten times higher, negative effects for the surface are expected after irradiation times of 6 min, cumulative. Therefore, for instruments using conversion surfaces it is essential to minimize the UV irradiation of conversion surfaces.

We also observed an increase in ionization efficiency with prolonged UV irradiation suggesting an actual improvement of the performance, which is attributed to the removal of water from the surface. This increase has to be accounted for when using the laboratory calibration of the conversion surfaces.

ACKNOWLEDGMENTS

This work is supported by the Swiss National Science Foundation.

[1] C. Auth, A. G. Borisov, and H. Winter, Phys. Rev. Lett. **75**, 2292 (1995).
[2] P. Stracke, F. Wiegershaus, S. Krischok, H. Müller, and V. Kempter, Nucl. Instrum. Methods Phys. Res. B **125**, 63 (1997).
[3] S. A. Deutscher, A. G. Borisov, and V. Sidis, Phys. Rev. A **59**, 4446 (1999).
[4] P. Roncin, J. Villette, J. P. Atanas, and H. Khemliche, Phys. Rev. Lett. **83**, 864 (1999).
[5] A. G. Borisov and V. A. Esaulov, J. Phys.: Condens. Matter **12**, R177 (2000).
[6] R. Souda, Int. J. Mod. Phys. B **14**, 1139 (2000).
[7] H. Winter, Phys. Rep. **367**, 387 (2002).
[8] J. A. Scheer, P. Wurz, and W. Heiland, Nucl. Instrum. Methods Phys. Res. B **212**, 291 (2003).
[9] J. A. Scheer, M. Wieser, P. Wurz, P. Bochsler, E. Hertzberg, S. A. Fuselier, F. A. Koeck, R. J. Nemanich, and M. Schleberger, Nucl. Instrum. Methods Phys. Res. B **230**, 330 (2005).
[10] J. A. Scheer, M. Wieser, P. Wurz, P. Bochsler, E. Hertzberg, S. A. Fuselier, F. A. Koeck, R. J. Nemanich, and M. Schleberger, Adv. Space Res. **38**, 664 (2006).
[11] P. Wurz, R. Schletti, and M. R. Aellig, Surf. Sci. **373**, 56 (1997).
[12] M. Wieser, P. Wurz, K. Brüning, and W. Heiland, Nucl. Instrum. Methods Phys. Res. B **192**, 370 (2002).
[13] P. Wurz, *The Outer Heliosphere: Beyond the Planets* (Copernikus Gesellschaft e.V., Katlenburg-Lindau, 2000), p. 251.
[14] T. E. Moore, D. J. Chornay, M. R. Collier, F. A. Herrero, J. Johnson, M. A. Johnson, J. W. Keller, J. F. Laudadio, J. F. Lobell, K. W. Ogilvie, P. Rozmarynowski, S. A. Fuselier, A. G. Ghielmetti, E. Hertzberg, D. C. Hamilton, R. Lundgren, P. Wilson, P. Walpole, T. M. Stephen, B. L. Peko, B. van Zyl, P. Wurz, J. M. Quinn, and G. R. Wilson, Space Sci. Rev. **91**, 155 (2000).
[15] P. Wurz, M. R. Aellig, P. Bochsler, A. G. Ghielmetti, E. G. Shelley, S. Fuselier, F. Herrero, M. F. Smith, and T. Stephen, Opt. Eng. **34**, 2365 (1995).
[16] D. J. McComas, F. Allegrini, P. Bochsler, M. Bzowski, M. Collier, H. Fahr, H. Fichtner, P. Frisch, H. O. Funsten, S. A. Fuselier, G. Gloeckler, M. Gruntman, V. Izmodenov, P. Knappenberger, M. Lee, S. Livi, D. Mitchell, E. Möbius, T. Moore, S. Pope, D. Reisenfeld, E. Roelof, J. Scherrer, N. Schwadron, R. Tyler, M. Wieser, M. Witte, P. Wurz, and G. Zank, Space Sci. Rev. **146**, 11 (2009).
[17] B. Schläppi, K. Altwegg, H. Balsiger, M. Hässig, A. Jäckel, P. Wurz, B. Fiethe, M. Rubin, S. A. Fuselier, J.-J. Berthelier, J. De Keyser, H. Rème, and U. Mall, "Influence of spacecraft outgassing on the exploration of tenuous atmospheres with *in situ* mass spectrometry," J. Geophys. Res. (in press).
[18] W. Zhou, Y. Yuan, and J. Zhang, J. Chem. Phys. **119**, 7179 (2003).

[19]P. Wurz and K. R. Lykke, J. Phys. Chem. **96**, 10129 (1992).
[20]M. Tulej, M. Iakovleva, I. Leya, and P. Wurz, "A miniature mass analyzer for *in situ* elemental analysis of planetary material: Performance studies," Anal. Bioanal. Chem. (2010) (in press).
[21]L. Floyd, Adv. Space Res. **23**, 1459 (1999).
[22]D. K. Prinz, C. W. Bowers, B. Lippey, and R. Goldberg, Bull. Am. Astron. Soc. **23**, 1038 (1991).
[23]A. Balogh, M. Bird, L. Blomberg, P. Bochsler, J.-L. Bougeret, J. Brückner, L. Iess, J. Guest, Y. Langevin, A. Milani, J.-A. Sauvaud, W. Schmidt, T. Spohn, R. von Steiger, N. Thomas, K. Torkar, H. Wänke, and P. Wurz, *BepiColombo - An Interdisciplinary Cornerstone Mission to the Planet Mercury; System and Technology Study Report* (ESA–SCI, Noordwjik, 2000), p. 1.
[24]R. G. Strom and A. L. Sprague, in *Solar System Update* (Springer, New York, 2006), pp. 55-85.
[25]J. Geiss and M. Witte, Space Sci. Rev. **78**, 229 (1996).
[26]S. Graf, K. Altwegg, H. Balsiger, P. Bochsler, B. Fiethe, and E. Montagnon, J. Spacecr. Rockets **45**, 57 (2008).
[27]S. Jans, P. Wurz, R. Schletti, T. Fröhlich, E. Hertzberg, and S. Fuselier, J. Appl. Phys. **87**, 2587 (2000).
[28]B. L. Peko and T. M. Stephen, Nucl. Instrum. Methods Phys. Res. B **171**, 597 (2000).
[29]T. M. Stephen and B. L. Peko, Rev. Sci. Instrum. **71**, 1355 (2000).
[30]P. Wurz, Keith R. Lykke, Michael J. Pellin, and Dieter M. Gruen, Vacuum **43**, 381 (1992).
[31]J. A. Scheer, K. Brüning, T. Fröhlich, P. Wurz, and W. Heiland, Nucl. Instrum. Methods Phys. Res. B **157**, 208 (1999).
[32]P. Wurz, T. Fröhlich, K. Brüning, J. Scheer, W. Heiland, E. Hertzberg, S. A. Fuselier, "Formation of Negative Ions by Scattering from a Diamond (111) Surface," *Proceedings of the Week of Doctoral Students 1998*, (edited by J. Safrankov and A. Kanka), Charles University, Prague, Czech Republic (Matfyzpress, Prague, 1998), pp. 257-262.
[33]E. V. P. Smith and D. M. Gottlieb, Space Sci. Rev. **16**, 771 (1974).
[34]T. N. Woods, D. K. Prinz, G. J. Rottman, J. London, P. C. Crane, R. P. Cebula, E. Hilsenrath, G. E. Brueckner, M. D. Andrews, O. R. White, M. E. VanHoosier, L. E. Floyd, L. C. Herring, B. G. Knapp, C. K. Pankratz, and P. A. Reiser, J. Geophys. Res. **101**, 9541 (1996).
[35]T. N. Woods, W. K. Tobiska, G. J. Rottman, and J. R. Worden, J. Geophys. Res. **105**, 27195 (2000).
[36]H. Koizumi, K. Shinsaka, T. Yoshimi, K. Hironaka, S. Arai, M. Ukai, M. Morita, H. Nakazawa, A. Kimura, Y. Hatano, Y. Ito, Y. Zhang, A. Yagishita, K. Ito, and K. Tanaka, Radiat. Phys. Chem. **32**, 111 (1988).
[37]J.-W. Shin and E. R. Bernstein, J. Chem. Phys. **130**, 214306 (2009).
[38]J. A. Scheer, P. Wahlström, and P. Wurz, Nucl. Instrum. Methods Phys. Res. B **256**, 76 (2007).
[39]S. Jans, P. Wurz, R. Schletti, K. Brüning, K. Sekar, W. Heiland, J. Quinn, and R. E. Leuchter, Nucl. Instrum. Methods Phys. Res. B **173**, 503 (2001).
[40]I. Batra, J. Phys. C **15**, 5399 (1982).
[41]V. M. Fomin, V. R. Misko, J. T. Devreese, and H. H. Brongersma, Nucl. Instrum. Methods Phys. Res. B **145**, 545 (1998).
[42]C. Auth, A. Mertens, H. Winter, A. G. Borisov, and V. Sidis, Phys. Rev. A **57**, 351 (1998).
[43]F. W. Meyer, Q. Yan, P. Zeijlmans van Emmichoven, I. G. Hughes, and G. Spierings, Nucl. Instrum. Methods Phys. Res. B **125**, 138 (1997).
[44]S. Ustaze, R. Verrucchi, S. Lacombe, L. Guillemot, and V. A. Esaulov, Phys. Rev. Lett. **79**, 3526 (1997).